Exploring plant-microbe interactions of the rhizobacteria Bacillus subtilis and Bacillus mycoides by use of the CRISPR-Cas9 system

Yi, Yanglei; Li, Zhibo; Song, Chunxu; Kuipers, Oscar P

Published in:
Environmental Microbiology

DOI:
10.1111/1462-2920.14305

Publication date:
2018

environmental microbiology

Environmental Microbiology (2018) **20**(12), 4245–4260 doi:10.1111/1462-2920.14305

Exploring plant-microbe interactions of the rhizobacteria *Bacillus subtilis* and *Bacillus mycoides* by use of the CRISPR-Cas9 system

Yanglei Yi, Zhibo Li, Chunxu Song and Oscar P. Kuipers*

Molecular Genetics, Groningen Biomolecular Sciences and Biotechnology Institute, University of Groningen, Groningen, The Netherlands.

Summary

***Bacillus subtilis* HS3 and *Bacillus mycoides* EC18 are two rhizosphere-associated bacteria with plant growth-promoting activity. The CRISPR-Cas9 system was implemented to study various aspects of plant-microbe interaction mechanisms of these two environmental isolates. The results show that fengycin and surfactin are involved in the antifungal activity of *B. subtilis* HS3. Moreover, this strain emits several other volatile organic compounds than 2,3-butanediol, contributing to plant growth promotion. Confocal laser scanning microscopy observations of the GFP-labelled strain showed that HS3 selectively colonizes root hairs of grass (*Lolium perenne*) in a hydroponic system. For *B. mycoides* EC18, we found that the wild-type EC18 strain and a Δ*asbA* (petropectin-deficient) mutant, but not the Δ*dhbB* (bacillibactin-deficient) and ADKO (*asbA* and *dhbB* double knockout) mutants, can increase the plant biomass and total chlorophyll. All the mutant strains have a reduced colonization capability on Chinese cabbage (*Brassica rapa*) roots, at the root tip and root hair region compared with the wild-type strain. These results indicate that the siderophore, bacillibactin, is involved in the plant growth promoting activity and could affect the root colonization of *B. mycoides.* Collectively, the CRISPR-Cas9 system we developed for environmental isolates is broadly applicable and will facilitate deciphering the mechanisms of *Bacillus*-plant interactions.**

Received 19 February, 2018; revised 31 May, 2018; accepted 4 June, 2018. *For correspondence. E-mail o.p.kuipers@rug.nl; Tel. +31 50 363 2093; Fax +31 50 363 2348.

Introduction

Plant growth-promoting rhizobacteria (PGPR) are soil bacteria that are able to colonize the surface of the root (and sometimes root inner tissues) and to stimulate plant growth and health (Vacheron *et al*., 2013). The use of PGPR as supplements to, or replacements of, chemical fertilizers or pesticides have steadily increased in the last decades (Adesemoye and Kloepper, 2009). A large diversity of bacterial species has been reported to have PGPR activity. *Bacillus* is one of the PGPR that received most extensive attention due to its specific metabolic and physiological traits including secretion of antimicrobial or signal peptides and formation of stress resistant-endospores (Kumar *et al*., 2011), which facilitate the formulation into commercial fertilizers or biocontrol agents.

B. subtilis is widely recognized as a model organism for studying plant-microbe interaction, because it was found in association with different plants as a good colonizer, which is highly important for biocontrol application. The colonization of *B. subtilis* on root surfaces involves chemotaxis and biofilm formation mechanisms (Beauregard *et al*., 2013; Allard-Massicotte *et al*., 2016). After colonization, *B. subtilis* benefits the plant growth in various ways, including suppressing plant pathogens by the secretion of antimicriobial compounds, such as fengycin (Romero *et al*., 2007) and/or the induction of systematic resistance (Ongena *et al*., 2007). Moreover, direct plant growth promotion effects can be achieved by the secretion of cytokine hormones and volatiles that modify plant hormone homeostasis. Apart from *B. subtilis*, other *Bacillus* species with biocontrol and plant growth promotion (PGP) potential have broadened the application capacity of this genus. For instance, the rhizosphere-associated *B. mycoides* can actively colonize root surfaces and form biofilm-like matrix, while some of the strains are even capable of entering root tissues and use an endophytic life strategy (Yi *et al*., 2017). It has been reported that *B. mycoides* increases disease resistance of sugar beet through the elicitation of systemic resistance (Bargabus *et al*., 2002) or oxidative burst (Bargabus *et al*., 2003) of the host. The biocontrol effects of *B. mycoides* against *Botrytis cinerea* and *Pythium*

aphanidermatum were confirmed in greenhouse conditions (Guetsky *et al*., 2002; Peng *et al*., 2017). Moreover, *B. mycoides* strains promote sunflower growth due to their nitrogen fixation activity (Ambrosini *et al*., 2016).

Although the significance of applying *Bacillus* with PGPR properties is being appreciated, the difficulty to study plant interaction mechanisms is hampered by the absence of an efficient genome editing system, for example, enabling gene deletion/inactivation/insertion in different *Bacillus* environmental isolates. Conventional methods for *Bacillus* gene inactivation based on single or double cross-over homologous recombination of a chromosomal gene by a mutated allele carried on a suicide vector require a relatively high transformation efficiency (Vagner *et al*., 1998; Zhang *et al*., 2015). This limitation hampers the application of this method since most of the undomesticated *Bacillus* strains are poorly naturally competent or otherwise hard to transform. To overcome this, a two-step system was developed for non-transformable *Bacillus,* which involved a second counter selection step by an antibiotic marker or a toxic gene (Suzuki *et al*., 2012; Dong and Zhang, 2014). However, those methods are still time-consuming and tedious since large-scale screening is needed for selecting desired double cross-over events. Apart from the homologous recombination mutagenesis methods, insertion-based mutagenesis including group II intron and transposon insertion normally either have low frequency or show a preference for a particular insertion motif (Shevchenko *et al*., 2002; Green *et al*., 2012; Saldanha *et al*., 2013). For these reasons, there is a strong necessity for developing a more efficient method for directed mutagenesis in environmental *Bacillus* species.

Clustered regularly interspaced short palindromic repeat (CRISPR) and the associated system is an adaptive immune system of bacteria and archaea against bacteriophages (Barrangou *et al*., 2007). The type II CRISPR system from *Streptococcus pyogenes* is the most compact CRISPR machinery by now and has been engineered to a precise genome editing tool (Jinek *et al*., 2012). This system has been adapted for targeted genome editing in not only eukaryotes, but also prokaryotes. For example, it has been successfully applied in a wide variety of bacteria including *Escherichia coli* (Li *et al*., 2015; Pyne *et al*., 2015), *S. pneumonia* (Jiang *et al*., 2013), *Lactobacillus reuteri* (Oh and van Pijkeren, 2014)*, Streptomyces* sp.(Tong *et al*., 2015), *Clostridium spp.* (Wang *et al*., 2016) and so forth. In *Bacillus*, such system has been developed for the model organism *B. subtilis* 168 by Altenbuchner (2016). The plasmid pJOE8999 contains a *cas*9 gene controlled by a mannose inducible promoter and a sgRNA driven by a constitutive promoter. A similar system has been developed for *B. subtilis* ATCC6051 (Zhang *et al*., 2016). A year after, Park and coworkers described a two-plasmid CRISPR-Cas9 system to delete large fragments of in the *B. subtilis* chromosome (So *et al*., 2017). However, those methods are developed either for model strains or for undomesticated strains with natural transformability.

B. subtilis HS3 and *B. mycoides* EC18 were isolated from grass rhizosphere and potato endosphere respectively. *B. subtilis* strain HS3 displays excellent antifungal and plant growth promoting activity, while *B. mycoides* EC18 has good endophytic and plant growth promotion potential. Both strains are recalcitrant to conventional genetic manipulation methods. Inspired by the high genome editing efficiency in prokaryotic organisms of the CRISPR-Cas9 system, we attempted to implement this system in these two rhizosphere-associated *Bacillus* strains. In order to further investigate the molecular mechanisms of their plant-microbe interactions, we describe a high efficient genome editing method based on the CRISPR-Cas9 system. By applying this method, we generated three and two mutants in *B. subtilis* HS3 and *B. mycoides* EC18, respectively, with potential relevance for their biocontrol abilities. Genetic, phenotypic and microscopic analyses were conducted to assess functions of the mutants during plant-*Bacillus* interactions.

Results and discussion

Implementation of CRISPR-Cas9 systems in *B. subtilis* HS3 and *B. mycoides* EC18

The all-in-one CRISPR-Cas9 genome editing system pJOE8999 has been established for the model strain of *B. subtilis* 168 previously (Altenbuchner, 2016). The shuttle vector pJOE8999 has a pUC minimal origin of replication (ori) to facilitate the cloning in *E. coli* and a gram-positive temperature permissive *ori* pET194^{TS}, which is permissive in *B. subtilis* below 37 °C and non-permissive above 42 °C. The *cas*9 gene is controlled by a mannose inducible promoter and the sgRNA is driven by a strong constitutive promoter. Although this system is highly efficient in *B. subtilis* 168 via natural transformation, the implementation of such system in an environmental Bacillus strain has not been reported. The gene deletion of this system depends on a double-cross-over allelic exchange event, which normally happens at a low frequency (Leloup *et al*., 1997). Since many environmental strains lack a functional competence system, electroporation was chosen to incorporate the plasmid into bacterial strains. In *B. subtilis* HS3, the transformation efficiency reached to $(4.2 \pm 1.1) \times 10^3$ cfu μg^{-1} DNA when using pNW33n plasmid. We transformed pJOE8999_gsigFHR into HS3 to delete the *sigF* gene. In order to increase the probability of double-cross-over events before the induction of *cas*9 gene, the cells were cultured overnight at 28 °C, 200 r.p.m. directly after electroporation in 1 ml

LBSP medium without antibiotic and mannose. After plating the transformed cultures on LB agar with 10 μg ml^{-1} kanamycin and 0.2% mannose, approximately 200 colonies were obtained per μg plasmid DNA. Colony PCR with primer HS3_sigFcheckF and HS3_sigFcheckR showed a 100% editing efficiency (number of colonies with desired fragment size/total colony checked; Supporting Information Fig. S2). The mutant was cured from plasmids and confirmed by PCR (Fig. 1A). Then, it was subjected to microscope observation for the sporulation ability. As shown in Fig. 1C and D, almost all wild-type cells complete the sporulation process and contain phase-bright forespores. In comparison, the mutant *B. subtilis* HS3Δ*sig*F cells have an abnormal morphology caused by a failure to form proper spores.

Genetic manipulation tools for *B. mycoides* have not been developed so far. Since the pJOE8999 system had high efficiency in the environmental isolate *B. subtilis* HS3, we developed a similar system, pYCR, for *B. mycoides* (Supporting Information Fig. S1). In order to knockout the *sigF* gene, plasmid pYCR_gsigFHR was transformed into *B. mycoides* EC18 by electroporation as described previously (Yi and Kuipers, 2017). The transformed cells were cultured in BHIS medium overnight and plated on LB agar plates with 100 μg ml^{-1} spectinomycin and 0.2% mannose. After incubation for 24 h at 30 °C, the transformants showed heterogeneity in colony size (Supporting Information Fig. S3). However, only the big colonies could grow when single colonies were inoculated into LB medium with 100 μg ml^{-1} spectinomycin. Thus, we speculated that the small colonies were possibly false positive colonies. Several 'true' transformants (big colonies) were checked by colony PCR with primers EC18_sigFcheckF and EC18_sigFcheckR. Ten out of thirteen colonies showed the expected mutant fragment size, which resulted in an editing efficiency of 77% (Supporting Information Fig. S2). The plasmid-cured mutant was confirmed by PCR and then grown in sporulation medium for microscopic observation. As shown in Fig. 1D and E, the EC18 wild-type strain has entered the last stage of sporulation

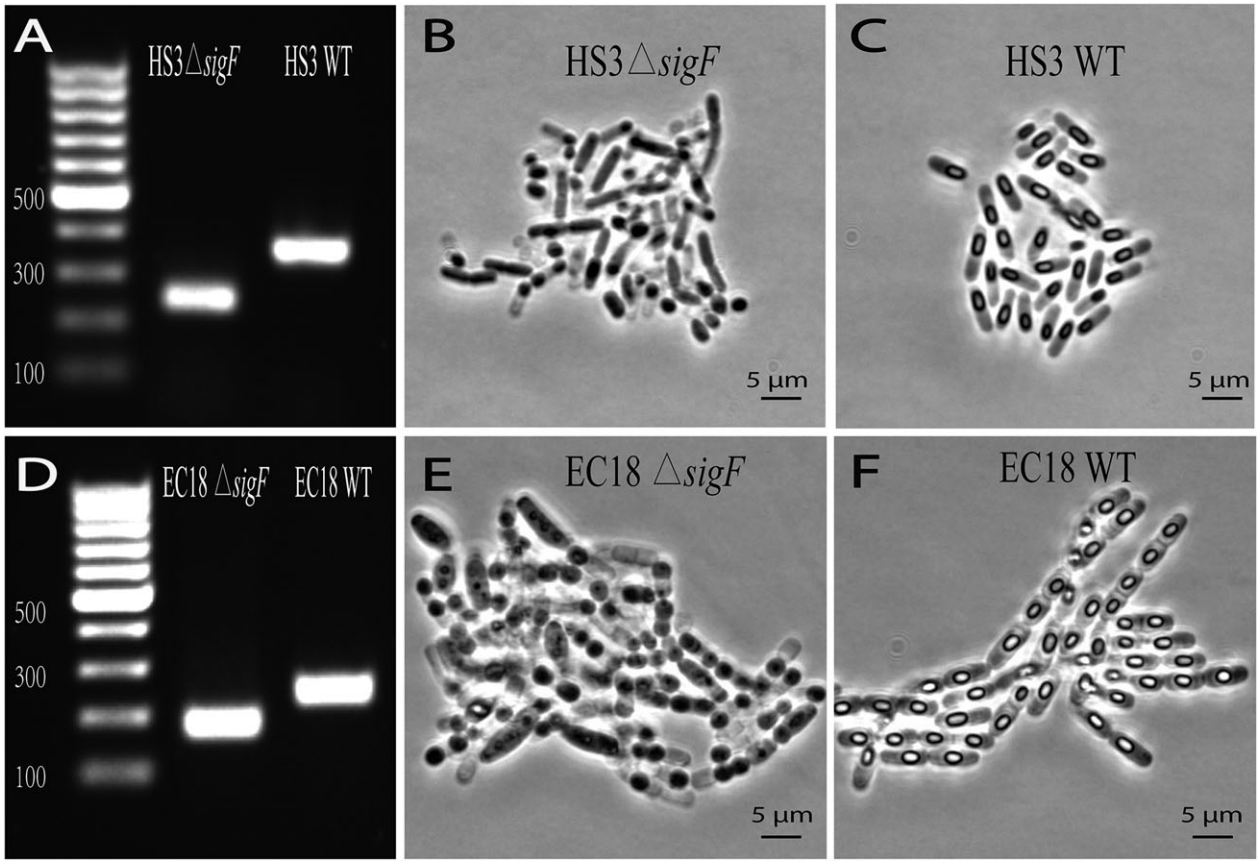

Fig. 1. CRISPR-Cas9-mediated knockout of *sigF* gene in *B. subtilis* HS3 and *B. mycoides* EC18.A. Colony PCR confirmation for the deletion of the 121-bp of the *sigF* gene in *B. subtilis* HS3.B, C. Microscopic observation of forespores formed by HS3Δ*sigF* and HS3 wild-type (WT) strains. Normal forespores were formed in HS3 WT and abnormal cell morphology was observed in the HS3Δ*sigF* mutant due to the deletion of *sigF.* D. Colony PCR confirmation for the deletion of the 60-bp of the *sigF* gene in *B. mycoides* EC18. (E-F) Microscopic observation of forespores formed by EC18Δ*sigF* and EC18 wild-type. Normal forespores were formed in EC18 WT, while an abnormal cell morphology was observed in the EC18Δ*sigF* mutant due to the deletion of *sigF.*

Table 1. Strains and plasmids used in this study.

Strains or plasmids	Relevant characteristic	Reference
Strains		
E. coli MC1061	F⁻, araD139, D(ara-leu)7696, D(lac)X74, *gal*U, *gal*K, hsdR2, *mcr*A, *mcr*B1, *rsp*L	Lab stock
B. subtilis HS3	isolated from grass rhizosphere	This study
B. mycoides EC18	isolated from potato endosphere	Yi *et al*. (2017)
B. subtilis HS3Δ*sig*F	HS3 derivative, Δ*sig*F	This study
B. subtilis HS3Δ*bdh*A	HS3 derivative, Δ*bdh*A	This study
B. subtilis HS3Δ*sfp*	HS3 derivative, Δ*sfp*	This study
B. subtilis HS3Δ*als*D	HS3 derivative, Δ*als*D	This study
B. subtilis HS3GFP	HS3 derivative, GFP inserted into the chromosome.	This study
B. mycoides EC18Δ*sigF*	EC18 derivative, Δ*sigF*	This study
B. mycoides EC18Δ*asbA*	EC18 derivative, Δ*asbA*	This study
B. mycoides EC18Δ*dhbB*	EC18 derivative, Δ*dhbB*	This study
B. mycoides EC18ADKO	EC18 derivative, Δ*asbA*, Δ*dhbB*	This study
B. mycoides EC18GFP	EC18 derivative, GFP inserted into the chromosome.	This study
B. mycoides EC18ΔA-GFP	EC18 derivative, Δ*asbA*, GFP inserted into the chromosome.	This study
B. mycoides EC18ΔD-GFP	EC18 derivative, Δ*dhbB*, GFP inserted into the chromosome.	This study
B. mycoides EC18ΔAD-GFP	EC18 derivative, Δ*asbA*, Δ*dhbB*, GFP inserted into the chromosome.	This study
Plasmids		
pJOE8999	PUC *ori*, kanR, rep pE194^{ts}, gRNA, P*man*-cas9.	Altenbuchner (2016)
pYCR	PUC *ori*, spec R, rep pWVO1^{ts}, gRNA, P*man*-cas9.	This study
PDR111_GFP(Sp)	bla amyE' Phyperspank, specR, lacI 'amyE	Overkamp *et al*. (2013)
pNW-sfGFP(SPS6)	*E. coli-Bacillus* shutter vector, P*pta*-sfGFP(SPS6), cmR	Yi *et al*. (2018)
PAW068	PUC *ori*, C9 transposase, rep pWVO1^{ts}, cmR, specR	Wilson *et al*. (2007)
pJOE8999_gsigFHR	pJOE8999 derivative, containing 20-nt spacer targeting *sig*F and fused up- and down- homologous fragment.	This study
pJOE8999_gsfpHR	pJOE8999 derivative, containing 20-nt spacer targeting *sfp* and fused up- and down- homologous fragment.	This study
pJOE8999_galsDHR	pJOE8999 derivative, containing 20-nt spacer targeting *alsD* and fused up- and down- homologous fragment.	This study
pJOE8999_gbdhHR	pJOE8999 derivative, containing 20-nt spacer targeting *bdhA* and fused up- and down- homologous fragment.	This study
pJOE8999_gamyGFP	pJOE8999 derivative, containing 20-nt spacer targeting α-amylase gene, and a *gfp* gene between the fused up- and down- homologous fragment.	This study
pYCR_gsigFHR	pYCR derivative, containing 20-nt spacer targeting *sig*F and fused up- and down- homologous fragment.	This study
pYCR_gasbHR	pYCR derivative, containing 20-nt spacer targeting *asbA* and fused up- and down- homologous fragment.	This study
pYCR_gdhbHR	pYCR derivative, containing 20-nt spacer targeting *dhbB* and fused up- and down- homologous fragment.	This study
pYCR_gamyGFP	pYCR derivative, containing 20-nt spacer targeting α-amylase gene, and a *gfp* gene between the fused up- and down- homologous fragment.	This study

and phase-bright forespores can be observed, while the mutant strain EC18Δ*sigF* showed an abnormal cell morphology and some cells lysed.

Fengycin and surfactin lipopeptides are involved in antifungal activity of B. subtilis *HS3*

Production of antimicrobials by rhizobacteria is one of the major mechanisms for its antagonistic activity against phytopathogens, and they have great application potential being used as biocontrol agents. It has been reported that lipopeptides are the main antifungal compounds produced by *Bacillus* during the interactions with fungi (Zihalirwa Kulimushi *et al*., 2017). Antagonistic experiments showed that *B. subtilis* HS3 has significant antifungal activity against several phytopathogenic fungi (data not shown). In order to investigate if lipopeptides are (partially) responsible for the antifungal activity, we knocked out the 4′-phosphopantetheinyl transferase encoding gene (*sfp*) which is required for the production of several lipopeptide antibiotics (Quadri *et al*., 1998). The editing plasmid pJOE8999_gsfpHR was transformed into HS3 by electroporation. The mutant colony was cured for plasmid and checked for the loss of a 188 bp fragment within the coding region of *sfp* gene by PCR with the primers HS3_sfpcheckF and HS3_sfpcheckR (Fig. 2A). The mutation of the *sfp* gene resulted in loss of lipopeptide production, which was confirmed by reversed phase-high-performance liquid chromatography (RP-HPLC; Fig. 2B). Furthermore, when the *sfp* gene was knocked out in HS3, antifungal activities were abolished against *Rhizoctonia solani* and *Fusarium culmorum*

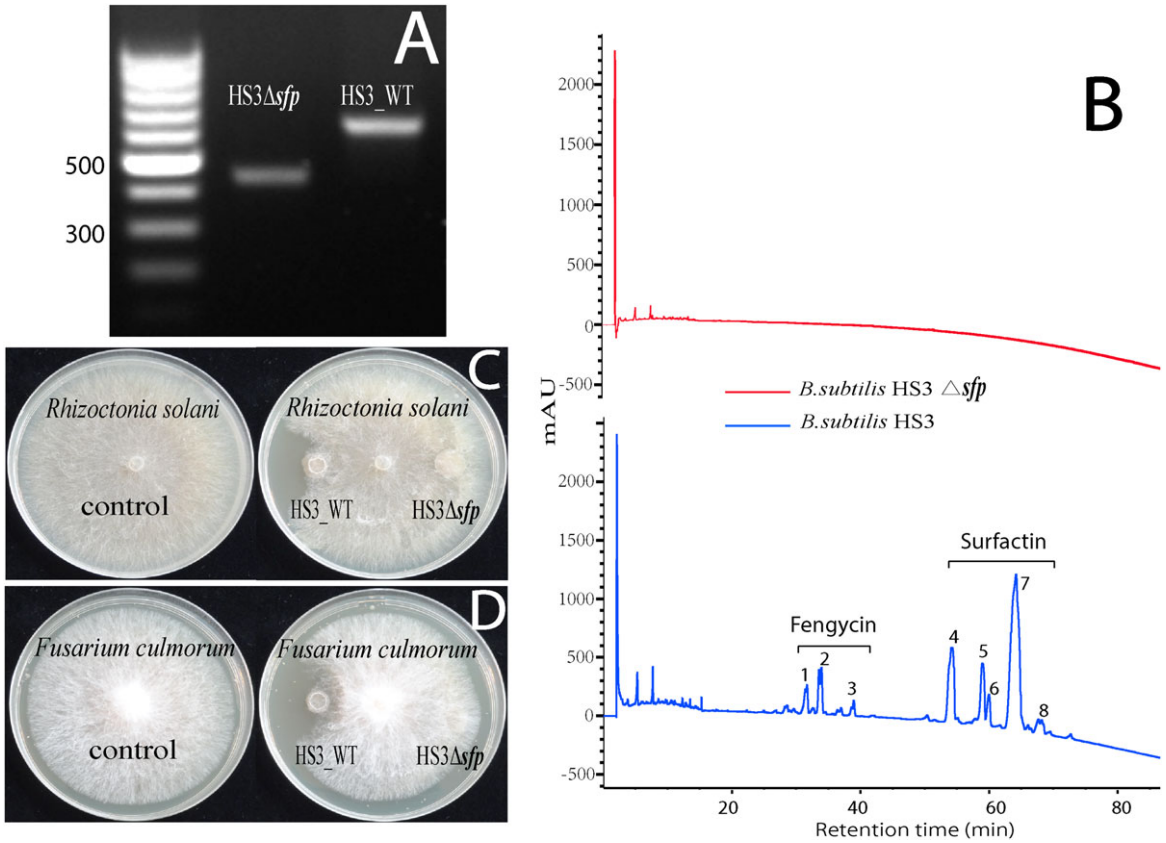

Fig. 2. Disruption of the *sfp* gene in *B. subtilis* HS3 by CRISPR-Cas9 system.A. Colony PCR confirmation for the deletion of the 188-bp of the *sfp* gene in *B. subtilis* HS3.B. Drop collapse assay with cell cultures of HS3 wild-type (WT) and Δ*sfp* mutant (HS3Δ*sfp*). Bacterial cells picked from a colony were suspended in sterile water to a final density of about 10^9 cells ml^{-1}, then 200 μl droplets were spotted on parafilm. Crystal violet was added to the droplets to facilitate visual assessment. A flat droplet is a highly reliable proxy for the production of the surface-active lipopeptides.C. Reversed phase-high-performance liquid chromatography chromatograms of cell-free culture extracts of wild-type HS3, and the HS3_Δ*sfp* mutant. The wildtype strain HS3 produces fengycin (retention time of approximately 32–40 min) and surfactin (retention time of approximately 55–68 min). AU stands for absorbance unit.D, E. Antifungal/oomycetal activities associated with lipopeptides production. Strain HS3 which has several lipopeptide biosynthetic clusters exhibited inhibition against *Rhizoctonia solani* and *Fusarium culmorum*. The HS3_Δ*sfp* mutant deficient in lipopeptides biosynthesis abolished the inhibition activities. Control is without bacteria.

(Fig. 2C and D). To characterize the lipopeptide compounds, mass spectra of the fractions collected from HPLC were subjected by MALDI-TOF analysis. The mass spectra of the eight peaks showed a series of the masses ranging from *m/z* value 1017.95 to 1543.21 (Supporting Information Fig. S4), which can be divided into two groups corresponding to fengycin (peak 1–3) and surfactin (peak 4–8) families of lipopeptides (Pathak and Keharia, 2014; Yang *et al*., 2015). These results confirmed the importance of fengycin and surfactin families of lipopeptides in the antifungal activity of HS3 against plant pathogens, which provide valuable information when further develop this strain into biocontrol agent.

Volatiles produced by *B. subtilis* HS3 promote grass growth

2,3-Butanediol is known to be a bacterial volatile organic compounds (VOC) that stimulate plant growth (Ryu *et al*., 2003). *B. subtilis* is capable of converting acetoin to 2,3-butanediol by the enzyme 2,3-butanediol dehydrogenase (BDH), which is encoded by the *bdhA* gene (Nicholson, 2008). The biosynthesis of acetoin involved the enzymes acetolactate synthase and acetolactate decarboxylase. The genes encoding these enzymes are *alsS* and *alsD* (Renna *et al*., 1993). In order to block the 2,3-butanediol, or both acetoin and 2,3-butanediol production in *B. subtilis* HS3, we deleted the *bdhA* and *alsD* gene by the editing vector pJOE8999_galsDHR and pJOE8999_gbdhHR respectively. After transformation, the colonies on LB-Km plates were checked by colony PCR. The primers HS3_alsDcheckF and HS3_alsDcheckR were used for HS3_Δ*als*D mutant, and the primers HS3_bdhAcheck-F and HS3_bdhAcheck-R were used for HS3_Δ*bdh*A mutant. As shown in Fig. 3A, both mutants showed the expected smaller fragment size than the wild-type. In order to detect the 2,3-butanediol production, wild-type and mutant strains were grown in LB medium containing 2% glucose, and the culture supernatant was run on silica gel TLC. A standard

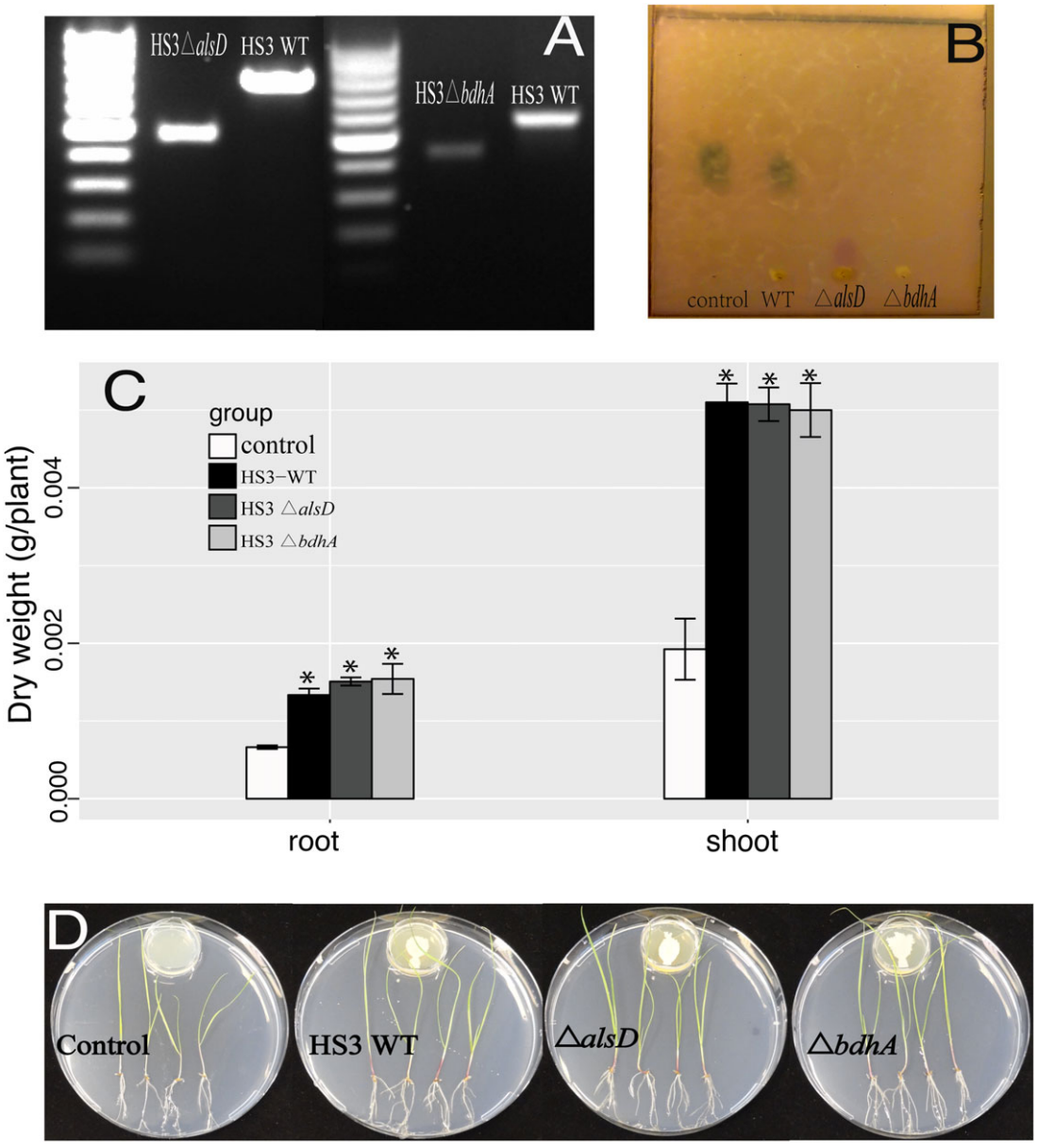

Fig. 3. Disruption of the *alsD* and *bhdA* gene in *B. subtilis* HS3 by CRISPR-Cas9 system. A. Colony PCR confirmation for the deletion of the 249-bp of the *alsD* gene and 138-bp of the *dhbA* gene in *B. subtilis* HS3.B. TLC detection of 2,3-butanediol from HS3 wild-type (WT), HS3_Δ*alsD* and HS3_Δ*bdhA*. Standard, 2,3-butanediol was included as a positive control.C, D. The biomass quantification and growth promotion of grass after 2 weeks of exposure to VOCs from HS3, HS3_Δ*alsD* and HS3_Δ*bdhA*. The two mutants as well as the wild type HS3 increase the biomass of grass by emitting VOCs.

2,3-butanediol was included as a control. The TLC results showed that the HS3 wild-type strain produced 2,3-butanediol, while the two mutants abolished the production (Fig. 3B). Grass seedlings (*Lolium perenne*) were exposed to VOCs produced by either wild-type HS3 or the mutants. Shoot and root biomass were increased approximately 2~3-fold compared with control plants for both wild-type HS3 and the mutants, and there was no significant difference between the wild-type strain and the mutants (Fig. 3C and D). Collectively, these results indicate that *B. subtilis* HS3 may emit other VOCs than 2,3-butanediol to mediate the growth of plants, which was beyond the scope of this study, but worthwhile to be further investigated in future work.

B. subtilis HS3 colonization of grass root observed by confocal laser scanning microscopy

The colonization of roots by rhizobacteria is the initial step in the interaction between beneficial bacteria and the host plant (Ahmad *et al*., 2011). Investigating the colonization

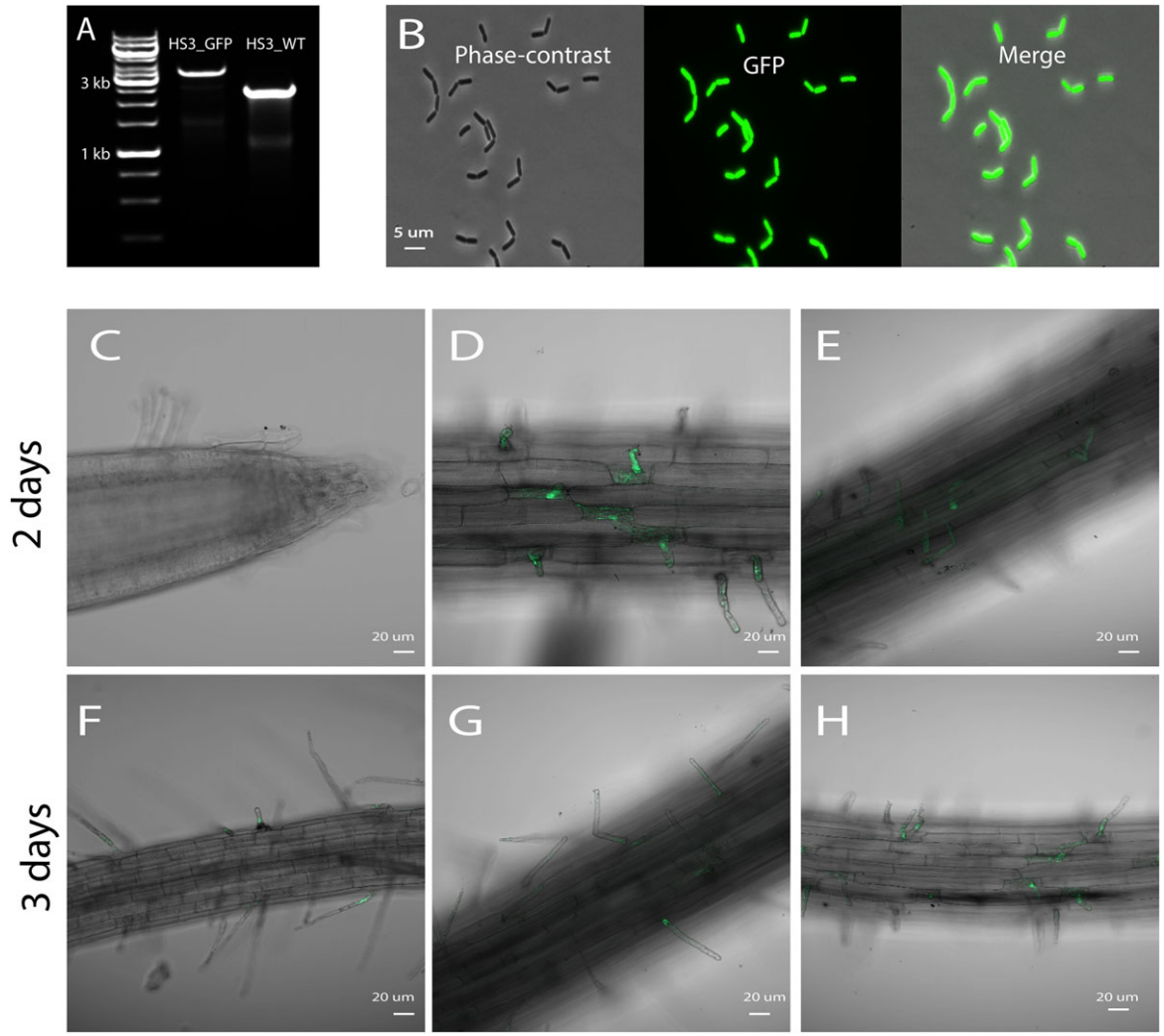

Fig. 4. Insertion of *gfp* gene into the chromosome of *B. subtilis* HS3 by CRISPR-Cas9 system and the observation of GFP-tagged cells in the grass rhizosphere from a hydroponic system.A. Colony PCR confirmation for the insertion of the *gfp* gene into *B. subtilis* HS3 chromosome.B. Fluorescent microscopic observation of the GFP-tagged HS3 cells. The HS3 GFP cells showed homogeneously green auto-fluorescence.C–H. *In planta* observation of *B. subtilis* HS3 cells in the rhizosphere of grass grown in a hydroponic system. Low amounts of colonization were found at the root tip, while strong colonization was exclusively observed at root hairs.

behaviour and establishment of bacteria in the root system is of great ecological interest. Moreover, monitoring inoculated bacteria is essential for the assessment of the effectiveness and consistent performance of inoculated PGPR. A prerequisite for such a study is the ability to track a specific microbe in the complex rhizosphere environment (Kluepfel, 1993). A classical approach is to introduce antibiotic resistance to the bacterium, then plate and enumerate the introduced bacterium on selective medium. However, this method is indirect and has several drawbacks including marker instability and high background from antibiotic resistance microbial populations (Benizri *et al*., 2001). *In situ* methods coupled with molecular techniques can better capture microbial activity and interactions with the host (Nawy, 2016). Fluorescent protein (FP) labelling system for *in situ* studies allows direct visualization of the tagged bacteria at the single-cell level, without the addition of exogenous substrates (Larrainzar *et al*., 2005). To study bacterial-host interactions, inserting the FP gene into bacterial chromosome provides an advantageous approach, since plasmid-based FP labelling is mostly instable, and the fluorescence signal show heterogeneously among different cells (Rodriguez *et al*., 2006). The CRISPR-Cas9 system is a convenient and efficient method to perform marker-free genome insertions.

In a previous study, we selected an optimized *gfp* for rhizosphere Bacilli (Yi *et al*., 2018). The optimized *gfp* was introduced to the editing plasmid, pJOE8999_gamyGFP, which was transformed into HS3 by electroporation. The chromosomal GFP insertion was confirmed by colony PCR with the primers HS3_GFPchechF and HS3_GFPchechR. The anticipated fragment size of 3399 bp was obtained (Fig. 4A). Fluorescent microscopy

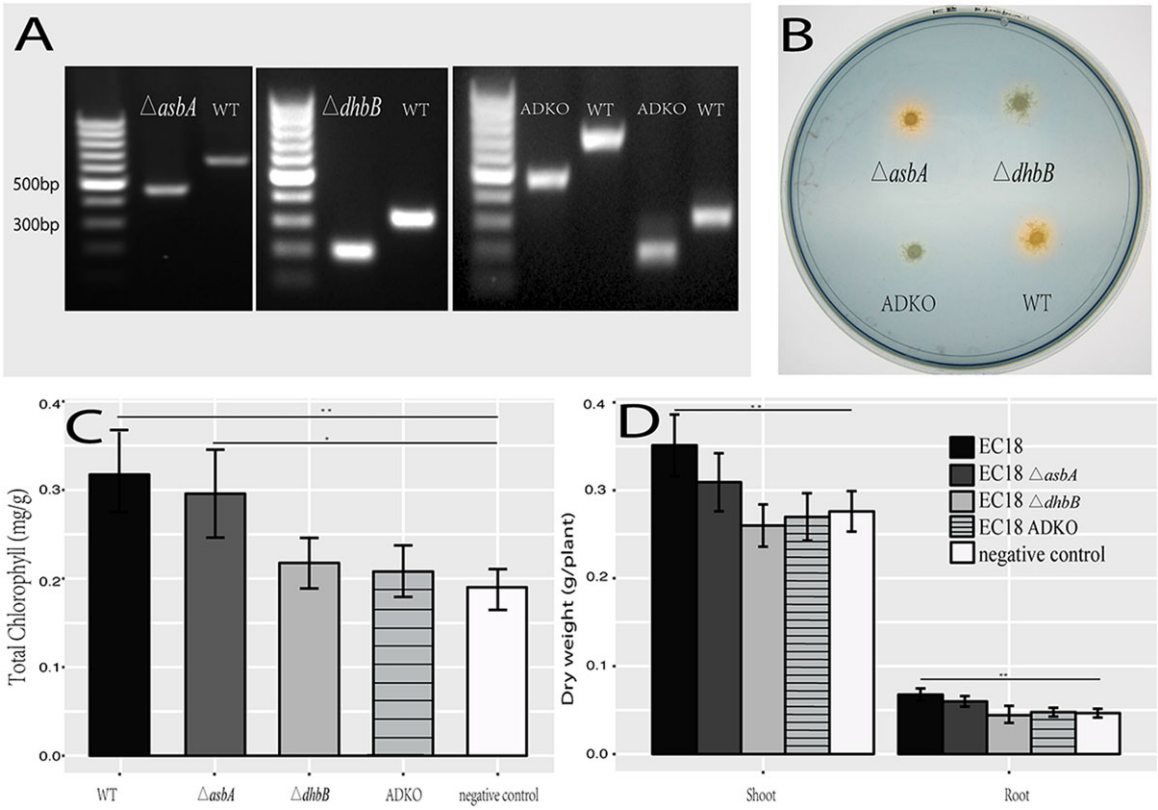

Fig. 5. Disruption of siderophore biosynthesis genes of *B. mycoides* EC18 by the CRISPR-Cas9 system.A. Colony PCR confirmation for the deletion of the 187-bp of *asb*A gene (Δ*asbA*), 115-bp of the *dhb*B gene (Δ*dhbB*) and the double deletion of these two genes in *B. mycoides* EC18 (ADKO).B. Siderophore detection by the O-CAS method. The yellowish halo indicates siderophore production.C. The total chlorophyll content of Chinese cabbage treated with *B. mycoides* EC18 wild-type and siderophore-deficient mutants, EC18Δ*asbA*, EC18Δ*dhbB* and the double mutant EC18ADKO.D. The biomass quantification of Chinese cabbage treated with *B. mycoides* EC18 wild-type and siderophore-deficient mutants.

showed that HS3_GFP cells were expressing GFP homogeneously (Fig. 4B). The GFP-labelled strain was inoculated with grass plants. After 2 and 3 days of inoculation, the intact grass roots were visualized by confocal laser scanning microscopy (CLSM) immediately after sampling. The *gfp*-tagged cells could be clearly detected on the root surface but not in all parts. No colonization was observed at the root tip (Fig. 4C). Interestingly, low colonization was observed at the older basal root parts. But strong colonization was only found on the root hairs (Fig. 4D–H). Similar bacteria colonization pattern was reported by Prieto *et al*. (2011) when *Pseudomonas* spp. was inoculated into olive roots.

Siderophores produced by *B. mycoides* promote the growth of iron-starved plants

Siderophores are low-molecular-weight iron chelators produced by bacteria and fungi under iron-limiting conditions and facilitate the solubilization and transport of iron into the cell by the cognate transport system (Schalk *et al*., 2011). Siderophores might also play an important role in plant-microbe interactions, since PGPR that produce siderophores combat the pathogenic microorganisms sequestering Fe^{3+} near the roots (Shilev, 2013). Moreover, the bacterial siderophores are often used by plants as iron source contributing to plant nutrition. For example, siderophores from strain *Chryseobacterium* C138 are effective in supplying Fe to iron-starved tomato plants by the roots (Radzki *et al*., 2013). The genome comparison analysis revealed two gene clusters responsible for siderophore biosynthesis in *B. mycoides* EC18: the *asb* operon for petrobactin and the *dhb* operon for bacillibactin (Supporting Information Fig. S5) and siderophore production was confirmed (Fig. 5B). It has been shown that petrobactin was required for *B. anthractis* growth both in iron-depleted conditions and in macrophages (Cendrowski *et al*., 2004). The presence of petrobactin biosynthesis gene (*asbA*) has been used as a marker gene for screening PGPR *Bacillus* (Lyngwi *et al*., 2016).

In order to determine whether petrobactin and bacillibactin are involved in the *B. mycoides*-plant interaction, we generated mutants of these two operons. The 20-nt

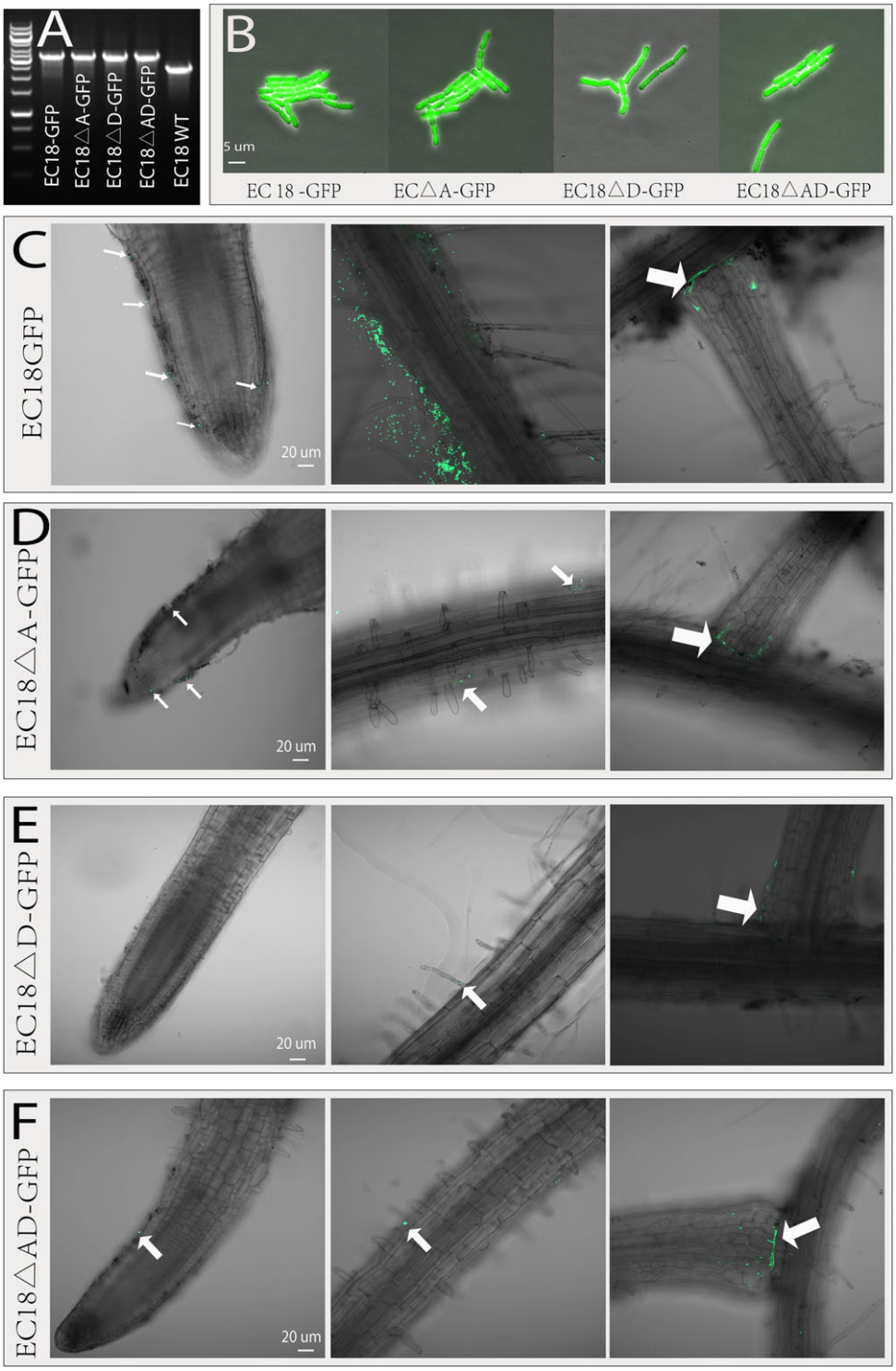

Fig. 6. Insertion of GFP into the chromosome of *B. mycoides* EC18 by CRISPR-Cas9 system and the observation of GFP-tagged cells in the rhizosphere of Chinese cabbage from a hydroponic system.A. Colony PCR confirmation for the insertion of the *gfp* gene in the chromosome *B. mycoides* EC18 and mutants.B. Fluorescent microscopic observation of the GFP-tagged *B. mycoides* wild-type and mutants cells. The EC18 WT as well as all the mutants' cells showed homogeneously green auto-fluorescence.C–F. *In planta* observation of *B. mycoides* wild-type and mutant cells colonized in the rhizosphere of Chinese cabbage grown in a hydroponic system.

spacer sequence was designed within the open reading frame of *asbA* and *dhbB* gene (Supporting Information Fig. S5). The spacer sequences as well as 1 kb flanking the up- and downstream region were introduced into pYCR to generate the editing plasmid pYCR_gasbHR and pYCR_gdhbHR. The editing plasmids were transformed into *B. mycoides* EC18, and the transformants on LB-SPEC100 (with 0.2% mannose) plates were checked by colony PCR to assess the successful knockout. The colonies with expected knockout size were cured from the plasmid, which resulted in the clean knockout strain *B. mycoides* EC18Δ*asbA* and *B. mycoides* EC18Δ*dhbB.* To make the *asbA* and *dbhB* double knockout strain *B. mycoides* ADKO, the plasmid pYCR_gdhbHR was transformed into the electro-competent cell of EC18Δ*asbA*, and the transformants were selected and confirmed as before. Colony PCR for Δ*asbA*, Δ*dhbB* and the double knockout mutant ADKO showed that all the mutants have expected smaller fragment sizes compared with the wild-type strain: 463 bp for EC18Δ*asbA* and 650 bp for EC18 wild type using primers EC18_asb_checkF and EC18_asb_checkR, and 184 bp for EC18Δ*dhbB* and 299 bp for EC18 wild type using primers EC18_dhb_checkF and EC18_dhb_-checkR (Fig. 5A). The siderophore production of all the mutants and the wild type were inspected by O-CAS agar (Fig. 5B). The production of siderophores by EC18Δ*asbA* is comparable to that of wild-type. In contrast, the EC18Δ*dhbB* had little production, and no siderophore production was detected from the double knockout EC18 ADKO. In the hydroponic system, the wild-type EC18 and the mutant EC18Δ*asbA* increased the total chlorophyll content of Chinese cabbage significantly. There were no significant differences of the total chlorophyll of the plants treated with EC18Δ*dhbB* and EC18 ADKO when compared with the control group (Fig. 5C). Biomass was also increased in the plants treated with wild type EC18 and EC18Δ*asbA*, with no significant difference between them. On the other hand, Δ*dhbB* mutant and double mutant ADKO abolished the plant growth promoting effect completely (Fig. 5D). These results indicate that bacillibactin is the main siderophore produced by *B. mycoides* and contributes to the plant growth promoting effects.

Siderophore-deficient strains show reduced plant colonization ability

Since the strain EC18Δ*dhbB* and EC18ADKO were unable to promote plant growth, we further compared their plant colonization capacity with the wild-type strain. The *gfp* gene with a strong constitutive promoter P*pta* was inserted into the chromosome of the strain EC18, EC18Δ*asbA*, EC18Δ*dhbA* and EC18ADKO to generate the GFP-tagged strain EC18-GFP, EC18ΔA-GFP, EC18ΔD-GFP and EC18ΔAD-GFP. All the strains were checked by PCR with the primers EC18_GFP_gcheckF and EC18_GFP_gcheckR binding the flanking region of the spacer sequence in the chromosome. The anticipated 3434 bp amplicon size (Fig. 6A) and homogeneous fluorescence of the cells (Fig. 6B) indicate the *gfp* insertion was successful and functional. The GFP-tagged strains were inoculated with the Chinese cabbage roots in a hydroponic system. After 2 days, the plant roots were collected for analysing *B. mycoides* colonization. The direct CLSM observation showed that the wild-type strain colonizes all plant root regions in a heterogeneous manner: a few cells colonize at the root tip, while most cells colonize the root hair initiation region, and a large number of cells aggregated at the junction region of main root and lateral root (Fig. 6C). The petropectin mutant strain EC18ΔA-GFP showed less colonization on the root tip and root hair region, compared with the wild-type control, while the lateral root emergence site was colonized by large bacterial populations (Fig. 6D). For the bacillibactin mutant EC18ΔD-GFP and the double knockout strain EC18ΔAD-GFP, the colonization of root tip and root hair regions was only occasionally observed. The cells of the two strains were arranged in microcolonies at the junctions of lateral roots with the primary roots (Fig. 6E &F).

The colonization of the wild-type *B. mycoides* and the siderophore-deficient strains were further compared at population level by colony counting assay. In line with the CLSM observation results, all mutant strains have a decreased ability to colonize plant roots compared with the wild-type EC18. The colonization rate of wild-type strain is more than twofolds higher than that of siderophore-deficient mutants (Supporting Information Fig. S6). The fate of the inoculated bacterial cells was followed by calculating the percentage of spores formed in the rhizosphere. About 19.1% of the total bacterial cells of the wild-type EC18 were heat-resistant spores, which was significantly higher than that in all mutant groups (Supporting Information Fig. S6).

In conclusion, we implemented the CRISPR-Cas9 system to perform gene knockout and chromosomal insertion in environmental *B. subtilis* HS3 and *B. mycoides* EC18 strains. The high efficiency in the two phylogenetically distant *Bacillus* species implies the great potential of the CRISPR-Cas9 system in genome editing of rhizosphere Bacilli. The generated mutants were used to study various traits in plant-microbe interactions. By interrupting the *sfp* gene in *B. subtilis* HS3, we demonstrated that the surfactin and fengycin family lipopeptides are responsible for the antagonistic activity against two relevant fungal pathogens. Moreover, we revealed that 2,3-butanediol is not the main VOC produced by HS3 to promote grass growth. Using a single-copy GFP-tagged

mutant, we showed that HS3 selectively colonizes on root hairs. In *B. mycoides* EC18, by interrupting two siderophore biosynthesis gene clusters via our CRISPR-Cas9 system, we highlighted the important role of petrobactin, in the plant growth promoting and root colonization.

Experimental procedures

Bacterial strains and growth conditions

Strains used in this study are shown in Table 1. *E. coli* MC1061 was used for plasmid construction. *B. subtilis* HS3 and *B. mycoides* EC18 were isolated from grass rhizosphere (Groningen, the Netherlands) and potato endosphere (Wijster, the Netherlands) respectively. *E. coli* and *B. subtilis* were grown in Lysogeny Broth (LB-Lennox: 1% Bacto-Tryptone, 0.5% Bacto-yeast extract, 0.5% NaCl) at 37 °C, 220 r.p.m. *B. mycoides* was grown in brain heart infusion (Bacto™ BHI, BD Bioscience, France) medium at 30 °C, 200 r.p.m. When required, antibiotics were added to the medium in the following final concentrations: 30 μg ml^{-1} or 10 μg ml^{-1} of kanamycin for *E. coli* and *B. subtilis* HS3 respectively. 100 μg ml^{-1} of spectinomycin for both *E. coli*, and *B. mycoides* EC18. 0.2% of mannose was added to the medium to induce the *cas9* expression. Solid media were prepared by adding 1.0% (wt/vol) agar (Bacto Agar, BD Bioscience, France).

DNA manipulation and oligonucleotides

Genomic DNA was isolated using GenElute bacterial genomic DNA kit (Sigma-Aldrich, USA) according to the manufacture's instruction. Plasmid DNA isolation, PCR products clean-up and gel extraction were performed using commercial NucleoSpin kits (Macherey-Nagel GmbH, Germany). Restriction, ligation, agarose gel electrophoresis and transformation of *E. coli* were performed as established protocols. Phusion (Thermo Scientific) polymerases were used for PCR to construct plasmid and DreamTaq polymerases DNA (Thermo Scientific) was used for colony PCR. Annealing reaction was carried out in annealing buffer containing 10 mM Tris (pH 8.0) and 50 mM NaCl with 10 μM of each oligonucleotide. Reaction tubes were heated to 95 °C for 5 min and cool to room temperature slowly. Oligonucleotides are listed in Supporting Information Table S1.

Plasmid construction

The plasmid pJOE8999 (Altenbuchner, 2016) was used for *B. subtilis* HS3 genome editing. For each mutant, the 20-nt protospacer sequence was designed by a web-based tool Benchling (https://www.benchling.com/) with *B. subtilis* 168 as reference genome and 'NGG' as PAM (Protospacer adjacent motif) sequence. The sequence with high on-target and off-target scores was chosen. As a proof of principle, the *sigF* gene was chosen because it is conserved in Bacilli. *sigF* encodes the forespore specific transcription factor σ^F that controls genes required for the early stages of prespore development (Hilbert and Piggot, 2004). To make a 121-bp deletion in the *sigF* gene, pJOE8999_gsigFHR was constructed in two steps. Plasmid pJOE8999 was first digested by BsaI resulting a 7423 bp fragment, which was ligated with the annealing product of primers HS3_gsigF_F and HS3_gsigF_R to generate plasmid pJOE8999_gsigF. A fragment of ~1 kb upstream and downstream of the spacer sequence was amplified by HS3_sigFHR1_F & HS3_sigFHR1_R and HS3_sigFHR2_F & HS3_sigFHR2_R primer sets respectively. The two fragments were connected by overlap PCR with the primers HS3_sigFHR1_F and HS3_sigFHR2_R, then digested with SfiI, purified and ligated into pJOE8999_gsigF to give plasmid pJOE8999_gsigFHR. In a similar way, pJOE8999_gbdhHR, pJOE8999_galsDHR, pJOE8999_gsfpHR vectors were constructed with designed primers (see Supporting Information Table S1) to make *bdhA*, *alsD* and *sfp* gene knockout mutant. To insert a GFP into the genome, an α-amylase gene was chosen as integration location. pJOE8999_gamy vector was constructed by inserting HS3_gamy_F and HS3_gamy_R annealing product into BsaI site. Then a 2259 bp fragment including the whole α-amylase gene was amplified from the *B. subtilis* HS3 genome by primer set HS3_amy1F_sfiI & HS3_amy2R_sfiI and ligated into the SfiI site of pJOE8999_gamy to obtain pJOE8999_gamyFL. The pJOE8999_gamyFL vector was used as a template to be amplified by primers HS3_amy1R and HS3_amy2F. The resulting PCR product was ligated with a *gfp* fragment obtained from pNW33N_sfGFP(SPS6) by EcoRI and HindIII cutting to give pJOE8999_gamyGFP.

Since *B. mycoides* has a low thermotolerance at 37 °C, the temperature sensitive *ori* of pJOE8999 was changed from pET194ts to PWVO1, which is amplification permissive at 30 °C and non-permissive at 37 °C. The pJOE8999 backbone without pET194ts was amplified by primers pJOE-PET194_F and pJOE-PET194_R and the PWVO1 *ori* was amplified by primer PWV01_F and PWV01_R from plasmid PAW068. The two fragments were connected by Quick-fusion cloning to generate pJOE-PWVO1. Plasmid pYCR was constructed by isolating the SpecR cassete as a 1025 bp XhoI/PstI fragment from PDR111_GFP(Sp) (Overkamp *et al*., 2013) and ligating it with the XhoI/PstI-digested pJOE-PWVO1. The construction scheme of the CRISPR/CAS plasmid pYCR used in *B. mycoides* is shown in Supporting Information Fig. S1. When designing the 20-bp protospacer sequence in Benchling, the *B. mycoides* ATCC6462

genome was used as reference and 'NGG' as PAM. As a proof-of-principle trial, a 60-bp deletion of *sig*F gene was achieved using plasmid pYCR_gsigFHR. The procedure to produce pYCR_gsigFHR was the same as that described for pJOE8999_gsigFHR. Plasmid pYCR was first digested with *Bsa*I and ligated with the oligo annealing product of EC18_gsigF_F and EC18_gsigF_R to get the plasmid pYCR_gsigF. Then a ~2 kb fragment combined with an upstream and a downstream fragment of the *sig*F spacer sequence was inserted at the SfiI site of pYCR_gsigF to generate pYCR_gsigFHR. In a similar way, vector pYCR_gasbHR, pYCR_gdhbHR and pYCR_gamyGFP were constructed. For GFP insertion at the α-amylase gene locus, the vector pYCR_gamyGFP was generated with the same procedure as for pJOE8999_gamyGFP. All the plasmids are listed in Supporting Information Table S1.

Electroporation and mutant generation

The electroporation factors including growth media, growth stage, electroporation buffer, pulse strength and recovery incubation time were optimized step-by-step for *B. subtilis* HS3. Briefly, one *B. subtilis* HS3 colony was inoculated in LBSP medium (LB medium supplemented with 50 mM KH_2PO_4 and K_2HPO_4, and 0.5 M sorbitol) overnight, then diluted 50 times in LBSP medium until the OD_{600nm} reached 0.65. The cell culture was centrifuged 10 min at 4000 g, 4 °C and the supernatant was discarded. The cell pellet was washed with pre-chilled electroporation buffer (0.25 M sorbitol in 10% glycerol solution) for 4four times and suspended in 1 ml electroporation buffer. 100 μl aliquots were flash frozen in liquid nitrogen and stored at – 80 °C until use. For *B. mycoides* EC18, the electroporation was performed as described previously (Yi and Kuipers, 2017).

About 1–2 μg plasmids were added into *B. subtilis* HS3 or *B. mycoides* EC18 electro-competent cells and exposed to a single pulse in a Gene Pulser System (Bio-Rad, USA) with the settings 25 μF, 10 kV cm^{-1}, 200 Ω. After electroporation, 1 ml growth media were directly added to the cells and incubated for 16–18 h at 28 °C, 200 r.p.m. The whole cultures were then plated on LB plate with corresponding antibiotic (10 μg ml^{-1} kanamycin for HS3 and 100 μg ml^{-1} spectinomycin for EC18) and 0.2% mannose to activate the *cas*9 gene expression. After incubation at 28 °C for 24 h, potential mutants were randomly picked and subjected to colony PCR with primers binding the flanking region of deletion or insertion sites on the genome (Supporting Information Table S1). A control was included using the genomic DNA as a template for PCR. PCR products were purified and verified by DNA sequencing. Colonies showing expected knockout band size were grown in LB liquid media with appropriate antibiotic and 0.2% mannose at 28 °C, 200 r.p.m. overnight to remove any unedited cells. Edited bacterial cells carrying the knockout plasmid were inoculated into growth medium (LB for *B. subtilis* and BHI for *B. mycoides*) without antibiotic and grown at plasmid replication-defective temperatures (45 °C for *B. subtilis* and 37 °C for *B. mycoides*) to stationary phase. Two more rounds of growth were conducted by diluting the stationary phase culture into fresh medium. Then a serial dilution of the culture was plated on LB agar plates in the absence of antibiotics and incubated at plasmid replication-defective temperatures overnight to curing the plasmid. Plasmid-cured candidates were identified by the loss of antibiotic resistance.

Microscopy

For microscopic observation of sporulating cells of *B. subtilis* HS3 and *B. mycoides* EC18, the wildtype strains, as well as their *sigF* gene mutant HS3Δ*sigF* and EC18Δ*sigF* were first grown on LB agar plates for overnight at 30 °C. A single colony was inoculated into Schaeffer's sporulation medium (Schaeffer *et al*., 1965) at 30 °C, 200 r.p.m. After growing for 30 h to a late stage of sporulation, 1 μl of the diluted culture was loaded on a 1.0% agarose microscopy slide. Samples were observed by a Nikon Ti-E microscope equipped with a CoolsnapHQ2 camera, a 40× phase contrast objective, and an Intensilight light source. Pictures were taken with 0.35 s of exposure for phase contrast.

For the detection of fluorescent signals of the GFP insertion mutant, cells were grown in LB liquid medium overnight at 30 °C, 200 r.p.m. One microliter of the diluted cell cultures was observed as described before. Pictures were taken with the following settings: 0.35 s of exposure for phase contrast, 2 s exposure for fluorescence at 440–490 nm excitation via a dichroic mirror of 495 nm and an emission filter at 500–505 nm. The final pictures were generated by ImageJ software.

HPLC and MALDI-TOF

Lipopeptides were extracted as previously described (Vater *et al*., 2002). Briefly, *B. subtilis* HS3 and its *sfp* mutant were grown in 200 ml LB broth at 28 °C, 220 r.p.m. for overnight. The supernatant was collected by centrifugation (10000 × g, 10 min) and acidify by adding 6 M HCl to a final pH of 2.0. After overnight acidify at 4 °C, the precipitation was collected by centrifugation (5000 × g, 20 min) and extracted with 10 ml methanol for 2 h. The crude extracts were filter sterilized with 0.45 μm Durapore™ membrane.

To check the lipopeptide extraction, crude extracts were subjected to HPLC equipped with Aeris wide pore

3.6u XB-C18 250 × 4.6 mm column. Eluent A was Mili-Q water with 0.1% trifluoroacetic acid (TFA); eluent B was HPLC-grade acetonitrile with 0.1% TFA. In each run, 100 μl crude extract was injected and eluted by a two-step gradient from 5% to 45% eluent B in 20 min and from 45% to 95% eluent B in 75 min (20 to 95 min).

Peaks only existed in *B subtilis* HS3 wild-type strain and these were collected for MALDI-TOF analysis. Samples of 0.5 μl were spotted and dried on the target. Subsequently, 0.5 μl of matrix solution (5 mg/ml α-cyano-4-hydroxycinnamic acid dissolved in 50% acetonitrile containing 0.1% TFA) was spotted on top of the sample. Mass spectra were obtained using a Voyager DE PRO MALDI-TOF mass spectrometer (Applied Biosystems).

Antifungal test

The fungi were inoculated in PDA agar plate and incubated at 28 °C for 5 days. An agar plug (5 mm diameter) with fungal hyphae was then inoculated into a new PDA agar plate. To prepare bacteria inoculums, an overnight culture of *B. subtilis* HS3 and its *sfp* mutant were pelleted and suspended in sterile MQ water to a final OD600nm of 1.0. Subsequently, 5 μl of each inoculum was spotted 2 cm away from the fungi plug symmetrically. Plates were sealed with parafilm and incubated at 28 °C for 5 days.

Effects of bacterial VOCs on plants and 2,3-butanediol detection

To determine the effects of VOCs on the growth of perennial ryegrass (*Lolium perenne*), seedlings were exposed to the VOCs emitted by the wild-type *B. subtilis* HS3 or the mutants in a dual-dish plates system. The dual-dish plates were prepared with a small petri dish containing LB (with 1% glucose) agar fixed in a large round petri dish containing ½ MS agar (Duchefa Biochemie). For surface sterilization, grass seeds were pre-treated with 0.3 M HCl for 6 h, followed by a 5 min bath in 2% sodium hypochlorite and then rinsed with sterile water for 10 times. The sterile seeds were sown on wet filter paper in a square plate, which was sealed with parafilm and then incubated at 25 °C in the dark. After sown and germination for 5 days, the grass seedlings were then transferred to dual dish plates on ½ MS medium. After 2 days, 5 μl overnight bacterial culture (diluted to OD600 = 1.0) was inoculated on LB medium in the dual-dish plates. Plates were sealed with parafilm and incubated in the climate chamber (25/21 °C of day/night, 16/8 h of day/night, 120 μmol m^{-2} s^{-1}, 70% humidity). After 7 days, the plant dry weights were measured.

The production of 2,3-butanediol in the *B. subtilis* HS3 culture was detected by thin layer chromatography (TLC) as described before (Saran *et al*., 2014). Briefly, the bacteria were grown in 10 ml Erlenmeyer flasks containing LB medium supplemented with 1% glucose at 30 °C, 150 r.p.m. for 48 h. The culture was then collected and centrifuged at 10 000 × g for 10 min to spin down the cells. The supernatant was spotted on silica gel TLC plates and use 70:30:1.5 of the hexane: ethyl acetate:glacial acetic acid as the mobile phase. Butanediol was visualized after the plates were sprayed with vanillin reagent and incubated at 100 °C until the spots were visible.

Siderophore detection

Siderophore detection assay was performed using the overlay chrome azurol S (O-CAS) method (Pérez-Miranda *et al*., 2007). Iron-deprived LB medium was made by stirring 5 g chelex 100 resin (Sigma, USA) with 100 ml LB for 1 h. Strains were inoculated on iron-deprived LB agar plate at 30 °C overnight. The overlay CAS was applied to the plates and a change in colour was observed after a period of 1 h.

Effects of a siderophore-producing/-deficient strain on iron-starved plants

Chinese cabbage seeds were first washed with sterilized water to remove dust and particles. The seeds were then immersed in 2%–3% sodium hypochlorite for 5 min and rinsed with distilled water. Finally, seeds were dipped in 70% ethanol for 2–3 min followed by thorough rinsing with sterile water. The surface sterilized seeds were aseptically placed on 25% iron-deprived Hoagland medium solidified with 1% agar. The plates were incubated for germination and growth in a climate chamber (21 °C, 16/8 h of day/light, ~120 μmol m^{-2} s^{-1}, 72% humidity) for 1 week. The seedlings were transferred to a 3 L hydroponic system containing 25% Hoagland's solution (without EDTA as chelate agent) and continued to grow for 2 days. Hoagland solution was aerated by air pump through a 0.45 μm filter membrane. 10 ml of *B. mycoides* wild-type or mutant strain in exponential growth phase were collected by centrifugation at 10 000 × g for 1 min. The cell pellet was resuspended in sterile water and added to the hydroponic system with final concentration of 2–3 × 10^4 CFU/ml cells. After 2 weeks of co-culturing, plants were harvested and the fresh and dry weight of root and shoot were measured. The total chlorophyll content was determined according to the method of Arnon (1949).

Monitoring of bacterial colonization on plant roots

Grass seeds were germinated on wet filter paper under sterile conditions as described before. The seedlings were transferred to a hydroponic system containing 1 l of ½ MS liquid medium and grown for 2 days. Then, the overnight culture of *B. subtilis* HS3_GFP was centrifuged at 10 000 r.p.

m. for 1 min. The cell pellet was suspended with ½ MS and inoculated to grass plants at a final concentration of 10^4 CFU ml^{-1}. After 2 and 3 days of co-culturing with bacteria, root samples were used for observation by a confocal laser scanning microscope (CLSM, LSM 800, Carl Zeiss, Germany). The CLSM was equipped with diode lasers and GaAsP detector. Images for fluorescence and bright field light channels were taken simultaneously. The CLSM settings were adjusted as follows: 0.2% power of the 488 nm laser line was set for excitation and 509–546 nm was set as emission wavelength. The pinhole size was 25 μm and pixel scanning time was 2.06 μs. The line scanning time was 2.47 ms with a line averaging of 2.

GFP labelled *B. mycoides* EC18 wild-type and siderophore deficient mutants were visualized in the rhizosphere of Chinese cabbage. Seven days old iron-starved seedlings were transferred to 25% Hoagland (EDTA was omitted) and grown for 2 days. *B. mycoides* EC18-GFP, EC18ΔA-GFP, EC18ΔD-GFP and EC18ΔAD-GFP were grown overnight. Bacterial cells were collected at 10000 r.p.m. for 1 min and then inoculated to Chinese cabbage plants at a final concentration of 10^4 CFU ml^{-1}. After 2 days of inoculation, the bacterial colonization of the wild type and mutant strains was compared at single cell level by CLSM observation, and at population level by colony counting. The colony counting assay was carried out as described by Dietel *et al*. with some modifications (Dietel *et al*., 2013). Briefly, roots were rinsed by sterile PBS before transferred into a 1.5 ml Eppendorf tube containing 1 ml PBS. A mild sonication treatment (4 rounds of 3 × 10 pulses of 1 s with an amplitude of 30%; Vibra CellTM, VCX 130, Sonics and Materials, Newtown, CT, USA) was applied to detach the cells from roots. The roots were then dipped on a dry, sterile filter paper to remove the remaining PBS and the fresh weight was recorded. The suspension was serially diluted and plated on LB agar plates. In parallel, a portion of the suspension was heated at 70 °C for 15 min prior to plating to calculate the number of bacterial spores in the rhizosphere. The plates were incubated at 30 °C overnight and the colony-forming unit (CFU) was counted.

Acknowledgements

We thank Dr. Auke van Heel in our group for his suggestions and comments on the manuscript. Y. Yi and Z. Li were financially supported by the Chinese Scholarship Council (CSC). C. Song was financially supported by Dutch NWO-TTW program Back to the Roots. The authors declare no conflict of interest.

References

Adesemoye, A.O., and Kloepper, J.W. (2009) Plant-microbes interactions in enhanced fertilizer-use efficiency *Appl Microbiol Biotechnol*. **85**: 1–12.

Ahmad, F., Husain, F.M., and Ahmad, I. (2011). In *Rhizosphere and root colonization by bacterial inoculants and their monitoring methods: a critical area in PGPR research*, Ahmad, F. (ed). In Microbes and Microbial Technology, New York, NY, USA: Springer, pp. 363–391.

Allard-Massicotte, R., Tessier, L., Lecuyer, F., Lakshmanan, V., Lucier, J.F., Garneau, D., *et al*. (2016) *Bacillus subtilis* early colonization of *Arabidopsis thaliana* roots involves multiple chemotaxis receptors. *mBio* **7**: e01664-16 *mBio*. **7**: e01664-16.

Altenbuchner, J. (2016) Editing of the *Bacillus subtilis* genome by the CRISPR-Cas9 system *Appl Environ Microbiol*. **82**: 5421–5427.

Ambrosini, A., Stefanski, T., Lisboa, B.B., Beneduzi, A., Vargas, L. K., and Passaglia, L.M.P. (2016) Diazotrophic bacilli isolated from the sunflower rhizosphere and the potential of *Bacillus mycoides* B38V as biofertiliser *Ann Appl Biol*. **168**: 93–110.

Arnon, D.I. (1949) Copper enzymes in isolated chloroplasts. Polyphenoloxidase in *Beta vulgaris Plant Physiol*. **24**: 1.

Bargabus, R., Zidack, N., Sherwood, J., and Jacobsen, B. (2002) Characterisation of systemic resistance in sugar beet elicited by a non-pathogenic, phyllosphere-colonizing *Bacillus mycoides*, biological control agent *Physiol Mol Plant Pathol*. **61**: 289–298.

Bargabus, R.L., Zidack, N.K., Sherwood, J.E., and Jacobsen, B.J. (2003) Oxidative burst elicited by *Bacillus mycoides* isolate bac J, a biological control agent, occurs independently of hypersensitive cell death in sugar beet *Mol Plant Microbe Interact*. **16**: 1145–1153.

Barrangou, R., Fremaux, C., Deveau, H., Richards, M., Boyaval, P., Moineau, S., *et al*. (2007) CRISPR provides acquired resistance against viruses in prokaryotes *Science*. **315**: 1709–1712.

Beauregard, P.B., Chai, Y., Vlamakis, H., Losick, R., and Kolter, R. (2013) *Bacillus subtilis* biofilm induction by plant polysaccharides *Proc Natl Acad Sci USA*. **110**: E1621–E1630.

Benizri, E., Baudoin, E., and Guckert, A. (2001) Root colonization by inoculated plant growth-promoting Rhizobacteria *Biocontrol Sci Technol*. **11**: 557–574.

Cendrowski, S., MacArthur, W., and Hanna, P. (2004) *Bacillus anthracis* requires siderophore biosynthesis for growth in macrophages and mouse virulence *Mol Microbiol*. **51**: 407–417.

Dietel, K., Beator, B., Budiharjo, A., Fan, B., and Borriss, R. (2013) Bacterial traits involved in colonization of *Arabidopsis thaliana* roots by *Bacillus amyloliquefaciens* FZB42 *Plant Pathol J*. **29**: 59–66.

Dong, H., and Zhang, D. (2014) Current development in genetic engineering strategies of *Bacillus* species *Microb Cell Fact*. **13**: 63.

Green, B., Bouchier, C., Fairhead, C., Craig, N.L., and Cormack, B.P. (2012) Insertion site preference of mu, Tn5, and Tn7 transposons *Mobile DNA*. **3**: 3.

Guetsky, R., Elad, Y., Shtienberg, D., and Dinoor, A. (2002) Improved biocontrol of *Botrytis cinerea* on detached strawberry leaves by adding nutritional supplements to a mixture of *Pichia guilermondii* and *Bacillus mycoides Biocontrol Sci Technol*. **12**: 625–630.

Hilbert, D.W., and Piggot, P.J. (2004) Compartmentalization of gene expression during *Bacillus subtilis* spore formation *Microbiol Mol Biol Rev*. **68**: 234–262.

Jiang, W., Bikard, D., Cox, D., Zhang, F., and Marraffini, L.A. (2013) RNA-guided editing of bacterial genomes using CRISPR-Cas systems *Nat Biotechnol*. **31**: 233–239.

Jinek, M., Chylinski, K., Fonfara, I., Hauer, M., Doudna, J.A., and Charpentier, E. (2012) A programmable dual-RNA–guided DNA endonuclease in adaptive bacterial immunity *Science*. **337**: 816–821.

Kluepfel, D.A. (1993) The behavior and tracking of bacteria in the rhizosphere *Annu Rev Phytopathol*. **31**: 441–472.

Kumar, A., Prakash, A., and Johri, B. (2011) *Bacillus* as PGPR in crop ecosystem. *In Bacteria in Agrobiology: Crop Ecosystems*. Maheshwari, D.K. (ed). Berlin, Heidelberg: Springer, pp. 37–59.

Larrainzar, E., O'Gara, F., and Morrissey, J.P. (2005) Applications of autofluorescent proteins for *in situ* studies in microbial ecology *Annu Rev Microbiol*. **59**: 257–277.

Leloup, L., Ehrlich, S.D., Zagorec, M., and Morel-Deville, F. (1997) Single-crossover integration in the *Lactobacillus* sake chromosome and insertional inactivation of the *pts*I and *lac*L genes *Appl Environ Microbiol*. **63**: 2117–2123.

Li, Y., Lin, Z., Huang, C., Zhang, Y., Wang, Z., Tang, Y.J., *et al*. (2015) Metabolic engineering of *Escherichia coli* using CRISPR–Cas9 meditated genome editing *Metab Eng*. **31**: 13–21.

Lyngwi, N.A., Nongkhlaw, M., Kalita, D., and Joshi, S.R. (2016) Bioprospecting of plant growth promoting bacilli and related genera prevalent in soils of pristine sacred groves: biochemical and molecular approach *PLoS One*. **11**: e0152951.

Nawy, T. (2016) Capturing microbial interactions *Nat Methods*. **14**: 35–35.

Nicholson, W.L. (2008) The *Bacillus subtilis* ydjL (bdhA) gene encodes acetoin reductase/2, 3-butanediol dehydrogenase *Appl Environ Microbiol*. **74**: 6832–6838.

Oh, J.H., and van Pijkeren, J.P. (2014) CRISPR–Cas9--assisted recombineering in *Lactobacillus reuteri Nucleic Acids Res*. **42**: e131–e131.

Ongena, M., Jourdan, E., Adam, A., Paquot, M., Brans, A., Joris, B., *et al*. (2007) Surfactin and fengycin lipopeptides of *Bacillus subtilis* as elicitors of induced systemic resistance in plants *Environ Microbiol*. **9**: 1084–1090.

Overkamp, W., Beilharz, K., Detert Oude Weme, R., Solopova, A., Karsens, H., Kovacs, A.T., *et al*. (2013) Benchmarking various green fluorescent protein variants in *Bacillus subtilis*, *Streptococcus pneumoniae*, and *Lactococcus lactis* for live cell imaging *Appl Environ Microbiol*. **79**: 6481–6490.

Pathak, K.V., and Keharia, H. (2014) Identification of surfactins and iturins produced by potent fungal antagonist, *Bacillus subtilis* K1 isolated from aerial roots of banyan (Ficus benghalensis) tree using mass spectrometry *3 Biotech*. **4**: 283–295.

Peng, Y.H., Chou, Y.J., Liu, Y.C., Jen, J.F., Chung, K.R., and Huang, J.W. (2017) Inhibition of cucumber *Pythium* damping-off pathogen with zoosporicidal biosurfactants produced by *Bacillus mycoides J Plant Dis Protection*. **124**: 481–491.

Pérez-Miranda, S., Cabirol, N., George-Téllez, R., Zamudio-Rivera, L., and Fernández, F. (2007) O-CAS, a fast and universal method for siderophore detection *J Microbiol Methods*. **70**: 127–131.

Prieto, P., Schiliro, E., Maldonado-Gonzalez, M.M., Valderrama, R., Barroso-Albarracin, J.B., and Mercado-Blanco, J. (2011) Root hairs play a key role in the endophytic colonization of olive roots by *Pseudomonas* spp. with biocontrol activity *Microb Ecol*. **62**: 435–445.

Pyne, M.E., Moo-Young, M., Chung, D.A., and Chou, C.P. (2015) Coupling the CRISPR/Cas9 system with lambda red recombineering enables simplified chromosomal gene replacement in *Escherichia coli Appl Environ Microbiol*. **81**: 5103–5114.

Quadri, L.E., Weinreb, P.H., Lei, M., Nakano, M.M., Zuber, P., and Walsh, C.T. (1998) Characterization of Sfp, a *Bacillus subtilis* phosphopantetheinyl transferase for peptidyl carrier protein domains in peptide synthetases *Biochemistry*. **37**: 1585–1595.

Radzki, W., Gutierrez Manero, F.J., Algar, E., Lucas Garcia, J.A., Garcia-Villaraco, A., and Ramos Solano, B. (2013) Bacterial siderophores efficiently provide iron to iron-starved tomato plants in hydroponics culture *Antonie Van Leeuwenhoek*. **104**: 321–330.

Renna, M.C., Najimudin, N., Winik, L., and Zahler, S. (1993) Regulation of the *Bacillus subtilis alsS*, *alsD*, and *alsR* genes involved in post-exponential-phase production of acetoin *J Bacteriol*. **175**: 3863–3875.

Rodriguez, H., Mendoza, A., Antonia Cruz, M., Holguin, G., Glick, B.R., and Bashan, Y. (2006) Pleiotropic physiological effects in the plant growth-promoting bacterium *Azospirillum brasilense* following chromosomal labeling in the clpX gene *FEMS Microbiol Ecol*. **57**: 217–225.

Romero, D., de Vicente, A., Rakotoaly, R.H., Dufour, S.E., Veening, J.-W., Arrebola, E., *et al*. (2007) The iturin and fengycin families of lipopeptides are key factors in antagonism of *Bacillus subtilis* toward *Podosphaera fusca Mol Plant-Microbe Interact*. **20**: 430–440.

Ryu, C.M., Farag, M.A., Hu, C.H., Reddy, M.S., Wei, H.X., Paré, P.W., and Kloepper, J.W. (2003) Bacterial volatiles promote growth in *Arabidopsis Proc Natl Acad Sci USA*. **100**: 4927–4932.

Saldanha, R.J., Pemberton, A., Shiflett, P., Perutka, J., Whitt, J.T., Ellington, A., *et al*. (2013) Rapid targeted gene disruption in *Bacillus anthracis BMC Biotechnol*. **13**: 72.

Saran, S., Yadav, S., and Saxena, R. (2014) Development of a highly sensitive, fast and efficient screening technique for the detection of 2, 3-butanediol by thin layer chromatography *J Chromatogr Sep Tech*. **5**: 1.

Schaeffer, P., Millet, J., and Aubert, J.-P. (1965) Catabolic repression of bacterial sporulation *Proc Natl Acad Sci USA*. **54**: 704–711.

Schalk, I.J., Hannauer, M., and Braud, A. (2011) New roles for bacterial siderophores in metal transport and tolerance *Environ Microbiol*. **13**: 2844–2854.

Shevchenko, Y., Bouffard, G.G., Butterfield, Y.S., Blakesley, R.W., Hartley, J.L., Young, A.C., *et al*. (2002) Systematic sequencing of cDNA clones using the transposon Tn5 *Nucleic Acids Res*. **30**: 2469–2477.

Shilev, S. (2013)Soil Rhizobacteria regulating the uptake of nutrients and undesirable elements by plants . In *Plant Microbe Symbiosis: Fundamentals and Advances*, Arora, N. K. (ed). Springer India: New Delhi, India, pp. 147–167.

So, Y., Park, S.Y., Park, E.H., Park, S.H., Kim, E.J., Pan, J.G., and Choi, S.K. (2017) A highly efficient CRISPR-Cas9-mediated

large genomic deletion in *Bacillus subtilis Front Microbiol*. **8**: 1167.

Suzuki, H., Murakami, A., and Yoshida, K. (2012) Counter-selection system for *Geobacillus kaustophilus* HTA426 through disruption of *pyrF* and *pyrR Appl Environ Microbiol*. **78**: 7376–7383.

Tong, Y., Charusanti, P., Zhang, L., Weber, T., and Lee, S. Y. (2015) CRISPR-Cas9 based engineering of actinomycetal genomes *ACS Synth Biol*. **4**: 1020–1029.

Vacheron, J., Desbrosses, G., Bouffaud, M.-L., Touraine, B., Moënne-Loccoz, Y., Muller, D., *et al*. (2013) Plant growth-promoting rhizobacteria and root system functioning *Front Plant Sci*. **4**: 356.

Vagner, V., Dervyn, E., and Ehrlich, S.D. (1998) A vector for systematic gene inactivation in *Bacillus subtilis Microbiology*. **144**: 3097–3104.

Vater, J., Kablitz, B., Wilde, C., Franke, P., Mehta, N., and Cameotra, S.S. (2002) Matrix-assisted laser desorption ionization-time of flight mass spectrometry of lipopeptide biosurfactants in whole cells and culture filtrates of *Bacillus subtilis* C-1 isolated from petroleum sludge *Appl Environ Microbiol*. **68**: 6210–6219.

Wang, Y., Zhang, Z.T., Seo, S.O., Lynn, P., Lu, T., Jin, Y.S., and Blaschek, H.P. (2016) Bacterial genome editing with CRISPR-Cas9: deletion, integration, single nucleotide modification, and desirable "clean" mutant selection in *Clostridium beijerinckii* as an example *ACS Synth Biol*. **5**: 721–732.

Wilson, A.C., Perego, M., and Hoch, J.A. (2007) New transposon delivery plasmids for insertional mutagenesis in *Bacillus anthracis J Microbiol Methods*. **71**: 332–335.

Yang, H., Li, X., Li, X., Yu, H., and Shen, Z. (2015) Identification of lipopeptide isoforms by MALDI-TOF-MS/MS based on the simultaneous purification of iturin, fengycin, and surfactin by RP-HPLC *Anal Bioanal Chem*. **407**: 2529–2542.

Yi, Y., and Kuipers, O.P. (2017) Development of an efficient electroporation method for rhizobacterial *Bacillus mycoides* strains *J Microbiol Methods*. **133**: 82–86.

Yi, Y., de Jong, A., Frenzel, E., and Kuipers, O.P. (2017) Comparative transcriptomics of *Bacillus mycoides* strains in response to potato-root exudates reveals different genetic adaptation of endophytic and soil isolates *Front Microbiol*. **8**: 1487.

Yi, Y., Frenzel, E., Spoelder, J., Elzenga, J.T.M., Elsas, J.D. V., and Kuipers, O.P. (2018) Optimized fluorescent proteins for the rhizosphere-associated bacterium *Bacillus mycoides* with endophytic and biocontrol agent potential *Environ Microbiol Rep*. **10**: 57–74.

Zhang, Z., Ding, Z.T., Shu, D., Luo, D., and Tan, H. (2015) Development of an efficient electroporation method for iturin A-producing *Bacillus subtilis* ZK *Int J Mol Sci*. **16**: 7334–7351.

Zhang, K., Duan, X., and Wu, J. (2016) Multigene disruption in undomesticated *Bacillus subtilis* ATCC 6051a using the CRISPR/Cas9 system *Sci Rep*. **6**: 27943.

Zihalirwa Kulimushi, P., Arguelles Arias, A., Franzil, L., Steels, S., and Ongena, M. (2017) Stimulation of Fengycin-type antifungal lipopeptides in *Bacillus amyloliquefaciens* in the presence of the maize fungal pathogen *Rhizomucor variabilis Front Microbiol*. **8**: 850.

Supporting Information

Additional Supporting Information may be found in the online version of this article at the publisher's web-site:

Fig. S1. Construction scheme of the pYCR plasmid. The construction was started from pJOE8999 by replacing the $pE194^{ts}$ origin of replication (ori) with the pWVO1 ori. Then the kanamycin resistance gene was replaced by spectinomycin resistance gene.

Fig. S2. Colony PCR results of the Δ*sigF* knockout in the two stains. (A) *B. subtilis* HS3 transformed with pJOE8999_gsigFHR plasmid and (B) *B. mycoides* EC18 transformed with pYCR_gsigFHR plasmid were grown on LB agar plate supplemented with 0.2% mannose and appropriate antibiotics. Colonies were subjected for PCR with the primers listed in Supporting Information Table S1. A smaller amplicon indicates the correct knockout.

Fig. S3. *B. mycoides* EC18 colonies after being transformed with (A) pYCR and (B) pYCR_gsigFHR. The transformed EC18 cells were plated on LB plates containing 100 μg ml^{-1} spectinomycin and 2% mannose. The plates were incubated at 30 °C overnight.

Fig. S4. MALDI-TOF of the peaks collected from the crude extracts of *B. subtilis* HS3 culture. The main mass numbers of *m*/*z* were indicated.

Fig. S5. Comparison of the pectrobactin and bacillibactin biosynthesis gene cluster of *B. mycoides* EC18 with close related species. The design of the 20-nt spacer and homologous repairing fragment is shown.

Fig. S6. Root colonization rate of GFP-tagged *B. mycoides* wild-type and mutants on Chinese cabbage. Two days after inoculation, the number of colony-forming units (CFU) per mg root fresh weight was determined. The spores in the rhizosphere were counted when the bacterial suspension was treated at 70 °C for 15 min prior to plating on LB plates. The data were analysed using an ANOVA, which was followed by Fisher's least significant different test (Fisher LSD) with SPSS software. Differences were considered significant when $P < 0.05$.

Table S1. Oligonucleotides used in this study